Transformation of terahertz spectra emitted from dual-frequency femtosecond pulse interaction in gases

A. V. Borodin,[1] N. A. Panov,[1] O. G. Kosareva,[1] V. A. Andreeva,[1] M. N. Esaulkov,[1] V. A. Makarov,[1] A. P. Shkurinov,[1] S. L. Chin,[2] and X.-C. Zhang[3,4,*]

[1]Department of Physics and International Laser Center, Lomonosov Moscow State University, Moscow 119923, Russia

[2]Centre doptique, photonique et laser and Département de physique, Université Laval, Québec G1V0A6, Canada

[3]Wuhan National Laboratory for Optoelectronics, HUST, Wuhan 430074, China

[4]The Institute of Optics, University of Rochester, Rochester, New York 14627-0186, USA

*Corresponding author: zhangxc@rochester.edu

Received January 25, 2013; revised March 12, 2013; accepted March 22, 2013; posted March 25, 2013 (Doc. ID 184095); published May 27, 2013

We demonstrate that the two basic physical mechanisms of terahertz (THz) generation in a femtosecond filament, namely, the free electron photocurrent and the nonlinear polarization of neutrals, can be identified through the spectral analysis of THz radiation. The contribution from the photocurrent peaks at the units of THz, while the neutrals yield the peak at the tens of THz. We suggest the practical implementation of such spectral analysis by varying the initial transform-limited laser pulse duration. © 2013 Optical Society of America

OCIS codes: (260.3090) Infrared, far; (190.4380) Nonlinear optics, four-wave mixing; (320.6629) Supercontinuum generation; (350.5400) Plasmas.

http://dx.doi.org/10.1364/OL.38.001906

Gas is one of the most promising and convenient medium for generation of broadband pulsed terahertz (THz) radiation. The highest THz generation efficiency is reached in the case of high intensity dual-frequency femtosecond (fs) laser pulses [1]. The most important contribution to generation of low-frequency field is provided by the photocurrent of free charges [2,3], induced by photoionization, and the four-wave mixing process [1,4,5], which describes nonlinear response of bound electrons in a gas.

In this paper we show both theoretically and experimentally that the THz-range radiation produced by copropagating in nitrogen and air 800 and 400 nm high-intensity fs laser pulses consists of the contribution from both the free electron current and the nonlinear polarization of neutral molecules. The major contribution from free electrons is in the low-frequency part of the THz spectrum, while the higher-frequency part is dominated by the instantaneous and delayed Kerr nonlinear response of neutrals at the difference frequency. We consider numerically the nonlinear response of the medium to the dual-frequency Gaussian pulse:

$$\mathbf{E}(t) = e^{-t^2/2\tau_0^2}[\mathbf{E}_\omega \sin \omega_0 t + \mathbf{E}_{2\omega} \sin(2\omega_0 t + \psi)], \quad (1)$$

where ω_0 is the first harmonic frequency (corresponding to the wavelength of 800 nm), vectors $\mathbf{E}_\omega$ and $\mathbf{E}_{2\omega}$ are the amplitudes of the first and the second harmonics, respectively, ψ is the phase mismatch, and $2\tau_0$ is the pulse duration at e^{-1} level. The angle between $\mathbf{E}_\omega$ and $\mathbf{E}_{2\omega}$ is 55° for optimal THz generation efficiency.

When a 1–5 mJ, 800 nm, 30–120 fs pulse is focused into atmospheric pressure gases its intensity achieves 50 TW/cm^2 which corresponds to the clamping value in the filament [6]. Free electrons are produced due to the ionization and they oscillate coherently with laser field $\mathbf{E}(t)$. It results in the formation of transient photocurrent. The electrons born at the moment t' acquire the instant velocity $\mathbf{V}_e(t,t')$ by the time $t > t'$:

$$\dot{\mathbf{V}}_e(t,t') = (e/m)\mathbf{E}(t)\Theta(t-t') - \nu_c \mathbf{V}_e(t,t'), \quad (2)$$

where m and e are electron mass and charge, $\Theta(t)$ is step function, $\nu_c = 5$ THz [7] is the collision frequency, and $\mathbf{V}_e(t',t')$ is the initial velocity of a photoelectron. The values with dot are derivative on time t. The photocurrent density $\mathbf{J}(t)$ at the time t is given by

$$\mathbf{J}(t) = e\int_{-\infty}^{t} \mathbf{V}_e(t,t')\frac{dN_e(t')}{dt'}\mathrm{d}t', \quad (3)$$

where $dN_e(t')$ is the density of free electrons born at the time moment t', and where $N_e(t)$ is the total electron density at the time t. We assume $N_e(-\infty) = 0$. The radiative part of the photocurrent density $\dot{\mathbf{J}}(t)$ is given by

$$\dot{\mathbf{J}}(t) = (e^2/m)\mathbf{E}(t)N_e(t) - \nu_c \mathbf{J}(t) + e\mathbf{V}_e(t,t)\dot{N}_e(t), \quad (4)$$

$$\hat{F}(\dot{\mathbf{J}}) = \frac{\omega}{\omega + i\nu_c}\left(\frac{e^2}{m}\hat{F}(\mathbf{E}N_e) + e\hat{F}(\mathbf{V}_e(t,t)\dot{N}_e)\right), \quad (5)$$

where $N_e(t)$ is the total electron density at the time t, $\mathbf{V}_e(t,t)$ is the initial velocity of the electron born at the time t, $\hat{F}$ is Fourier transform operator, $S_{\mathrm{pc}}(\omega) = |\hat{F}(\dot{\mathbf{J}})|^2$ is the photocurrent spectral intensity, and ω is an angular frequency. In this work we consider the case of tunneling ionization to calculate N_e, and thus we take $\mathbf{V}_e(t,t) = 0$ [8].

The other mechanism is attributed to nonlinear response of bound electrons to a high-intensity laser field $\mathbf{E}(t)$. The contribution to the spectrum from neutral molecules is described by the third-order polarization $\mathbf{P}$, which is expressed through the light field as

$\mathbf{P}(t) = \chi^{(3)}_{1111}|\mathbf{E}(t)|^2\mathbf{E}(t)$. The value $\chi^{(3)}_{1111}$ is the third-order nonlinear susceptibility tensor component. The radiative part of this polarization is written as $\ddot{\mathbf{P}}$, while the spectral intensity $S_{\rm pol}$ is given by

$$\hat{F}(\ddot{\mathbf{P}}) = -\omega^2\chi^{(3)}_{1111}\hat{F}(|\mathbf{E}|^2\mathbf{E}), \qquad S_{\rm pol}(\omega) = |\hat{F}(\ddot{\mathbf{P}})|^2. \quad (6)$$

Our model is aimed at the clarification of the contribution of free and bound electrons to the THz radiation from filaments and can be used for THz spectra prediction in the propagation experiments through extended media. The model is complementary to the model [9], where THz wave is calculated exactly through the quantum mechanically obtained electron wave packet outgoing from a single atom under the action of ω and 2ω photons. The latter approach [9] might be used for the description of the laser pulse interaction with the low-pressure or gas jet targets where the propagation effects are not crucial.

Figure 1 shows the dependence of the simulated spectral intensity coming from the plasma photocurrent Figs. 1(a) and 1(b)] and the nonlinear polarization [Figs. 1(c) and 1(d)] on frequency $\nu = \omega/2\pi$. The pulse intensity is 100 TW/cm^2 and its duration is 32 fs [Figs. 1(a) and 1(c)] and 120 fs [Figs. 1(b) and 1(d)]. As shown in [2], the optimum phase mismatch ψ between ω and 2ω harmonics is $\pi/2$ for free electron response and 0 for bound electrons. This optimum phase mismatch causes maximum conversion to THz radiation. For all the conditions the spectral intensity has the distinct maxima at the fundamental, the second harmonic and the difference frequencies. The spectral width of THz radiation is scaled by the initial laser pulse as approximately $\propto \tau_0^{-1}$.

For the photocurrent case the spectrum is enriched with the continuum of frequencies forming a pedestal due to the strongly nonlinear dependence of the electron density N_e on the field intensity [Figs. 1(a) and 1(b)].

In the experiment we investigated the power spectral density of THz radiation for different pump pulse durations. We used conventional THz-TDS spectrometer layouts and four Ti:Sa laser oscillators with the transform-limited pulses with the durations: 32 fs (Coherent Legend Elite Duo), 40 fs (Spectra Physics Spitfire Pro), 85 fs (Spectra Physics Hurricane), and 120 fs (Spectra Physics Spitfire Pro). The central wavelength of all the laser systems was 800 nm, the repetition rate was 1 kHz

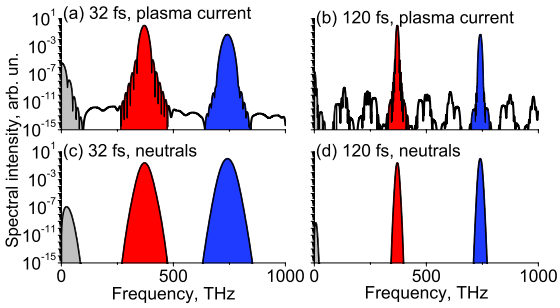

Fig. 1. Simulated spectra of the dual-frequency fs pulse (Eq. 1) producing filament in air. (a) and (b) Spectra calculated from the plasma current or (c) and (d) from the nonlinear polarization of neutrals.

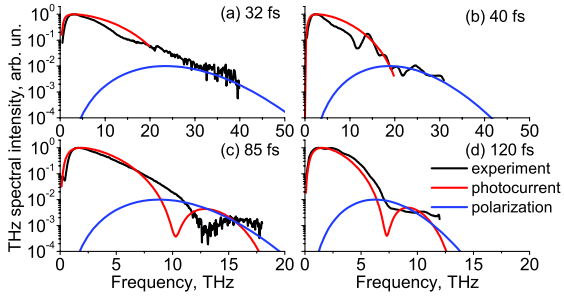

Fig. 2. Experimentally obtained in nitrogen and simulated spectra irradiated from either plasma current or the nonlinearity of neutrals. In the experiment the energy is 1 mJ and 100 μJ for ω and 2ω pulses, respectively.

and the pump energy used was about 1 mJ. The 100 μm I-type BBO crystals were used for the second harmonic generation and focal lengths of the focusing lenses was 15 cm. We used ambient air or pure nitrogen to decrease the water vapor absorption for both THz pulse generation and detection. The THz spectrum was obtained via THz-TDS [3] using the gases ionized by femtosecond pulses to generate the sense broadband terahertz pulses [10].

Comparison between the simulated from the photocurrent model and the experimentally obtained spectra shows good agreement in the maximum frequency position and the overall spectral width (Fig. 2, red and black curves). The agreement is in the range 1–10 THz, which is the evidence for the contribution from the photocurrent mechanism to the generation of THz signal registered in all four experimental setups.

The frequency $\nu^{\rm pc}_{\rm max} = \omega^{\rm pc}_{\rm max}/2\pi$, at which the maximum is attained, depends on the electron collision frequency and the pulse duration. The spectrum due to the photocurrent $S_{\rm pc}$ has the form

$$S_{\rm pc}(\omega) = \frac{\omega^2}{\omega^2 + \nu_c^2} \times f(\omega), \quad (7)$$

where $f(\omega) = |e^2\hat{F}(\mathbf{E}N_e)/m|^2$. Numerical simulations show that $f(\omega) \equiv S_{\rm pc}(\omega; \nu_c = 0)$ achieves its maximum value at $\omega = 0$. Thus, for $\omega \approx 0$ we can write the equation for f in the form $f(\omega) = \alpha(-\omega^2 + \beta^2)$, where α and β are positive constants. The product $\alpha\beta^2$ represents the value of spectral intensity maximum, and β corresponds to the spectral width, thus $\beta \propto \tau_0^{-1}$. By setting $dS_{\rm pc}/d\omega = 0$ we find the frequency, at which the photocurrent spectrum achieves its maximum $(\omega^{\rm pc}_{\rm max})^2 = \nu_c(\sqrt{\beta^2 + \nu_c^2} - \nu_c)$. For the broad THz spectrum $\beta \gg \nu_c$ this estimate yields $\omega^{\rm pc}_{\rm max} = \sqrt{\nu_c\beta}$ in agreement with [11].

The frequency, at which the spectrum maximizes, is $\nu^{\rm pc}_{\rm max} \propto \tau_0^{-1/2}$ and it agrees well with the experimental data in Fig. 3(a). The shape of the spectra simulated based on the assumption of the photocurrent model is in good agreement with the experimental results [Figs. 3(b) and 3(c)].

The spectra $S_{\rm pol}$ originating from the polarization of neutral molecules occupy the higher frequency range 5–50 THz as compared with the lower-frequency (1–10 THz) contribution from the photocurrent mechanism [Fig. 2, blue curves; Fig. 3(d)]. By repeating the

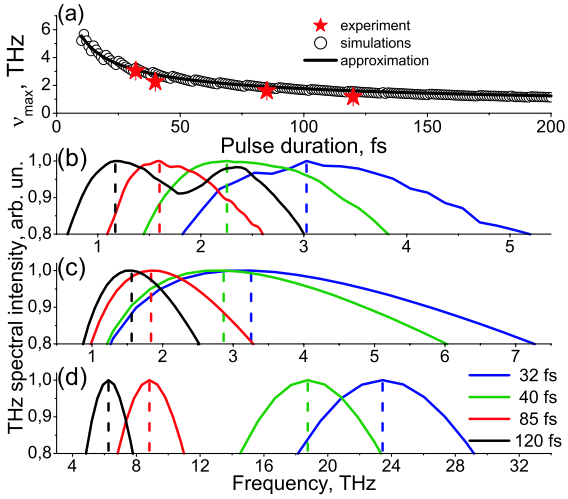

Fig. 3. (a) Frequency $\nu_{\max}$, at which the spectra take their maximum. (b) Experimentally obtained and (c) and (d) simulated spectra for different initial laser pulse duration. THz spectra from (c) free electron photocurrent and (d) Kerr-induced nonlinearity of neutrals.

calculations according to the Eq. (7) for the polarization-induced spectrum S_{pol} and setting $dS_{\text{pol}}/d\omega = 0$, we obtain the frequency, where the spectra originating from the polarization mechanism maximize $\nu_{\max}^{\text{pol}} \propto \tau_0^{-1}$. In our experiments the contribution to the higher-frequency part of the THz spectrum was lost due to the detection method oriented at its lower-frequency part. If the effect of the Kerr nonlinearity on the pulse propagation is increased by using the longer geometrical focusing distance and/or higher gas pressure in the cell, then the higher frequency part of THz spectrum is clearly pronounced [12]. It extends toward 40 THz and agrees with our simulation results [Fig. 2(b)].

The full 3D and time numerical simulations of filamentation show that at the beginning of the filament, where the maximum plasma density is attained, the low-frequency part of THz spectrum is formed in the vicinity of 10 THz. With propagation the Kerr nonlinearity of neutrals contributes to the four-wave mixing process [13].

In conclusion, we used four transform-limited pump pulses with different durations to measure the spectra of THz waves irradiated from the dual-frequency filament. The frequency, at which THz spectral maximum is attained in the experiment, as well as THz spectral width, increases with decreasing initial pulse duration.

We developed the model of THz generation, which takes into account the self-consistent plasma production in the dual-frequency laser field as well as the contribution of the third-order Kerr nonlinearity of neutrals. THz spectra, originating from these two physical mechanisms, are clearly separated in the frequency domain. The simulated photocurrent spectrum occupies 1–10 THz range. It is in agreement with the experimental data both on the position of the frequency, at which the spectral maximum is attained, and the spectral width as functions of the initial laser pulse duration.

We note that the frequency, at which the spectrum takes its maximum, increases as the square root of the inverse laser pulse duration if free electrons are mainly responsible for THz generation. However, if the third-order Kerr nonlinearity is responsible for THz generation, the frequency defining the spectral maximum, increases faster than in the photocurrent case and is directly proportional to the inverse pulse duration. In the experiment the contribution from neutral molecules to THz spectra is not clearly pronounced due to the detection method, which filters the higher frequencies out.

Thus, the frequency range of THz spectra and the rate of change of the spectral maximum position with the laser pulse duration serve as the indication of the physical mechanism dominating the dual-frequency pulse propagation in a gas. Simultaneously, the initial laser pulse duration is the tool for managing the width and the maximum position of THz radiation spectrum.

We acknowledge support from the RFBR (Grants 12-02-31894, 12-02-01368, 12-02-31341, and 12-02-33029), the Council of the President of the RF for Support of Young Scientists (N5996.2012.2), Leading Scientific Schools (6897.2012.2), Ministry of Education and Science of the RF (N8393), Dynasty Foundation, and Huazhong University of Science and Technology, Wuhan, China. We thank K. Wang and Q. Luo for assistance in the experiment.

References

1. D. J. Cook and R. M. Hochstrasser, Opt. Lett. **25**, 1210 (2000).
2. K. Y. Kim, J. H. Glownia, A. J. Taylor, and G. Rodriguez, Opt. Express **15**, 4577 (2007).
3. A. V. Balakin, A. V. Borodin, I. A. Kotelnikov, and A. P. Shkurinov, J. Opt. Soc. Am. B **27**, 16 (2010).
4. X. Xie, J. Dai, and X. C. Zhang, Phys. Rev. Lett. **96**, 075005 (2006).
5. Y. Chen, T.-J. Wang, C. Marceau, F. Théberge, M. Châteauneuf, J. Dubois, O. Kosareva, and S. L. Chin, Appl. Phys. Lett. **95**, 101101 (2009).
6. N. Karpowicz and X.-C. Zhang, Phys. Rev. Lett. **102**, 093001 (2009).
7. J. Kasparian, R. Sauerbrey, and S. L. Chin, Appl. Phys. B **71**, 877 (2000).
8. P. Sprangle, J. R. Penano, B. Hafizi, and C. A. Kapetanakos, Phys. Rev. E **69**, 066415 (2004).
9. S. L. Chin, in *Advances in Multi-Photon Processes and Spectroscopy* (World Scientific, 2004), Vol. **16**, p. 432.
10. N. Karpowicz, J. Dai, X .Lu, Y. Chen, M. Yamaguchi, H. Zhao, X.-C. Zhang, L. Zhang, C. Zhang, M. Price-Gallagher, C. Fletcher, O. Mamer, A. Lesimple, and K. Johnson, Appl. Phys. Lett. **92**, 011131 (2008).
11. N. Karpowicz, X. F. Lu, and X. C. Zhang, J. Mod. Opt. **56**, 1137 (2009).
12. G. Rodriguez and G. L. Dakovski, Opt. Express **18**, 15130 (2010).
13. L. Berge, S. Skupin, C. Kohler, I. Babushkin, and J. Herrmann, Phys. Rev. Lett. **110**, 073901 (2013).